

Experimental Study of Electro-Mechanical Dual Acting Pulley Continuously Variable Transmission Ratio Calibration

Bambang Supriyo*, Kamarul Baharin Tawi, Hishamuddin Jamaluddin, Mohamed Hussein

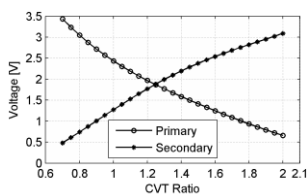
Faculty of Mechanical Engineering, Universiti Teknologi Malaysia, 81310 UTM Johor Bahru, Johor Malaysia

*Corresponding author: bambang@fkm.utm.my

Article history

Received 8 Jun 2014
Received in revised form 20 July 2014
Accepted 16 August 2014

Graphical abstract



Abstract

This paper presents an experimental study of Electro-mechanical Dual Acting Pulley (EMDAP) Continuously Variable Transmission (CVT) ratio calibration. When there is no slip between belt and pulley sheaves, the CVT ratio will be the same as the geometrical ratio of secondary to primary pulley radii as well as the primary to secondary speed ratio. In EMDAP CVT system, both primary and secondary DC motors are used to control the primary and secondary axial pulley positions to vary the primary and secondary pulley radii. In this case, the pulley radii can be measured indirectly using axial pulley position sensors. Calibration process is carried out by manually adjusting the geometrical ratio of secondary to primary radii based on measurements of primary and secondary pulley positions and validated with the primary to secondary speed ratio determined from primary (input) and secondary (output) shaft speed measurements for the CVT ratio range of 0.7 to 2.0. The calibration results are recorded and used as reference data for future EMDAP CVT calibration and ratio control developments.

Keywords: Geometrical ratio; speed ratio; CVT ratio; EMDAP CVT; CVT calibration; electro-mechanical CVT

© 2014 Penerbit UTM Press. All rights reserved

1.0 INTRODUCTION

Nowadays, transportations mainly contribute to the increase in the worldwide fossil-fuel based energy consumption and greenhouse gas (GHG) emissions which relate to world energy source depletion and environmental pollutions [1]. The pollutions potentially affect on global change in weather, also known as global warming or greenhouse effect phenomenon [2]. Stricter government regulations on energy efficiency and greener environment have been implemented to restrain the fuel consumption and emission growths, in which car manufacturers are required to produce vehicles with lower fuel consumptions and greenhouse gas emissions [3]. These requirements can be achieved by improving the overall vehicle efficiency, which generally highly depends on the engine efficiency. However, the engine itself is actually still not efficient, since only about 20-30% of the combustion energy becomes an effective power for mobility and accessories [4] and the rests are losses in the forms of heat, friction, etc. Therefore, the intensive researches in engine efficiency improvements still continue [5-11].

Since it is likely more difficult to get more efficiency out of the engine, the car manufacturers have become more interested in the development of new generation of highly efficient transmission which is combined with the engine and allows the

engine to always run within its most efficient operating range for various vehicle load conditions. A metal pushing V-belt continuously variable transmission (CVT) is a kind of transmission based on a set of primary (input) pulley, secondary (output) pulley and a metal belt running between the pulley gaps. Unlike manual transmission systems that rely on different sets of fixed gears, the CVT system provides an infinite number of transmission ratios between its lowest and highest ratio limits for changing the speed ratio between engine and drive wheel. This unique characteristic makes it possible for engine operating conditions to be adjusted accordingly to follow its maximum power or minimum fuel consumption driving strategy, hence making the engine to run efficiently [12] and improving the vehicle's overall efficiency and performance [13]. In addition, CVT offers a smooth driving comfort without shift-shock due to continuous shift and no torque interruption during shifting. Due to these features, CVT has gained its popularity as a promising transmission for future automotive applications [14].

Majority of belt type CVTs equipped in cars use hydraulic actuation system to supply pulley clamping forces for maintaining a constant ratio and preventing belt slip. The drawbacks of these CVTs are mostly related to high pump and high oil pressure of hydraulic system as well as belt loss [12, 15-16]. Continuous power consumption of hydraulic actuator in the CVT, especially

for constant transmission ratio application, introduces power loss that partially decreases the overall CVT efficiency.

A DC motor based electro-mechanical pulley actuating system of EMDAP CVT adopting power screw mechanism offers a viable solution to overcome constant ratio power loss experienced by hydraulic system. The DC motor systems actuate power screw mechanisms to adjust the axial positions of both primary and secondary pulley sheaves, hence indirectly adjusting the pulley radii and changing the CVT ratio. When the DC motor is turned off, the screw mechanism mechanically locks the current axial positions of primary and secondary pulley sheaves and keeps the CVT ratio constant without consuming energy.

Current researches in electro-mechanical CVTs, such as electro-mechanically actuated metal V-belt type Continuously Variable Transmission- EMPAct CVT [17], dry hybrid belt electro-mechanical CVT [18-19], and electro-mechanically actuated pulley (EMDAP) CVT [20-22], have been carried out to mature their concepts and technologies. Most of these current electro-mechanical CVTs use single movable pulley sheave on each of its pulley shaft. The application of single movable pulley sheave introduces belt misalignment. Application of belt misalignment for long period of time may damage the belt and pulley, which in turn worsening the CVT's performance, efficiency, reliability and safety [23]. Some studies involving various control strategies have been carried out lately to minimize the belt misalignment effects [24-25]. Unlike other electro-mechanical CVT systems, EMDAP CVT adopts two movable pulley sheaves on each of its primary and secondary pulley shafts to mechanically eliminate belt misalignment. These primary and secondary movable pulley sheaves always clamp the metal pushing V-belt in aligned condition.

This paper is an extended works of [26]. It focuses more on experimental works of EMDAP CVT ratio calibration within the ratio range of 0.7 to 2.0 by validating the geometrical ratio of secondary to primary radii determined from measurements of primary and secondary axial pulley positions with the primary to secondary speed ratio calculated from primary (input) and secondary (output) shaft speed measurements. The results of this calibration are recorded and used as reference data for future use in EMDAP CVT calibration and ratio control developments.

2.0 BASIC CVT RATIO

The basic CVT ratio adjuster is shown in Fig. 1. It consists of primary and secondary pulleys and a belt connecting the two pulleys. If the belt is inextensible and running on both pulleys' surfaces perfectly without slip, then tangential velocities (v_T) of both pulleys and the belt are the same.

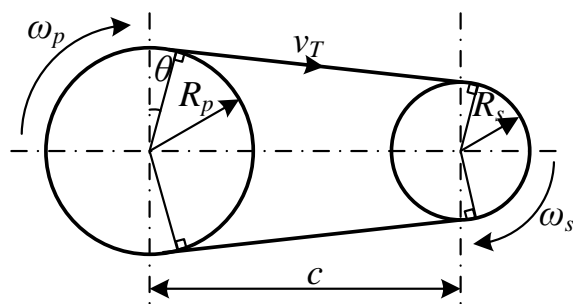


Figure 1 CVT ratio adjuster

The equations related to speed, running radii and ratios are given as follows:

$$\omega_s R_s = \omega_p R_p \quad (1)$$

$$r_{gsp} = R_s / R_p \quad (2)$$

$$r_{vps} = \omega_p / \omega_s \quad (3)$$

Where, R_p and R_s are primary and secondary pulley running radii, respectively, ω_p and ω_s are primary and secondary angular speeds, respectively, r_{gsp} is geometrical ratio of secondary to primary radii and r_{vps} is primary to secondary speed ratio. The CVT ratio in this study refers to the value which is the same as the values of both the primary to secondary speed ratio and the secondary to primary radii geometrical ratio, when there is no slip between pulleys and belt. The equations involving belt length, running radii and axial pulley positions are presented as follows:

$$L = (\pi + 2\theta)R_p + (\pi - 2\theta)R_s + 2c \cos(\theta) \quad (4)$$

$$R_p = R_s + c \sin(\theta) \quad (5)$$

$$X_p = (R_p - R_{p0}) \tan(\alpha) \quad (6)$$

$$X_s = (R_s - R_{s0}) \tan(\alpha) \quad (7)$$

where, L is belt length (645.68 mm), c is pulley center distance (165 mm), θ is half the increase in the wrapped angle on the primary pulley, R_{p0} and R_{s0} are minimum primary and secondary running radii, X_p and X_s are primary and secondary pulley positions and α is pulley wedge angle (11°).

By substituting R_p in (5) into (4) and setting various values of angle θ within its working range, it is possible to obtain the values of running radii R_s and R_p , respectively. By using (2), the CVT ratio can be determined, then the values of angle θ can be limited to the range that satisfies CVT ratio of 0.7 to 2.0, and the relationship between running radii and CVT ratio can be established as shown in Fig. 2.

Next, by using (6) and (7), the relationship among axial pulley positions X_p , X_s and CVT ratio can also be established as shown in Fig. 3. Based on this relationship, the desired CVT ratio can be set using the predetermined values of primary and secondary axial pulley positions, and conversely, the actual CVT ratio can be determined using (2), by first obtaining the values of axial pulley positions X_p and X_s from pulley position measurements and calculating the values of running radii R_s and R_p using (6) and (7). In real time application, axial pulley positions are sensed using linear position sensors and shaft speeds are detected using incremental encoder speed sensors. The CVT ratio, represented by primary to secondary speed ratio, is determined using (3).

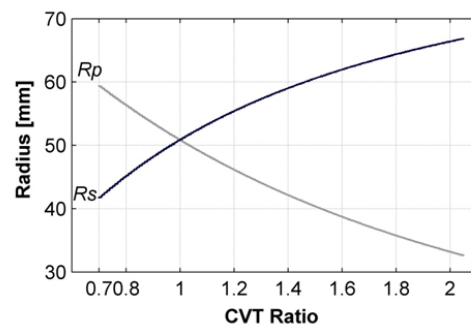


Figure 2 Relationship between running radii and CVT ratio

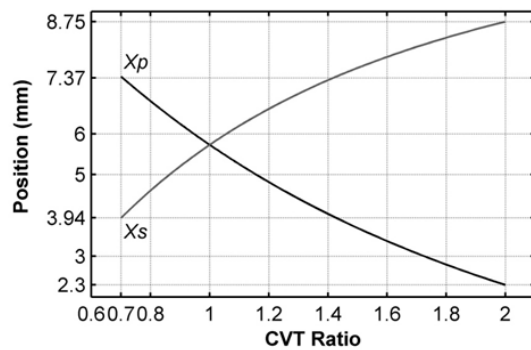


Figure 3 Relationship between pulley positions and CVT ratio

3.0 EMDAP CVT SYSTEM

The EMDAP CVT system, as shown in Fig. 4, consists of primary (input) pulley set, secondary (output) pulley set and a Van Doorne's metal pushing V-belt connecting the two pulleys. Each pulley set consists of two movable pulley sheaves facing to each other which can be axially shifted along its respective shaft. By utilizing these two movable pulley sheaves, the belt misalignment can be eliminated, since the belt is always clamped in alignment condition in any CVT ratio. By applying sufficient belt-pulley clamping force, the belt transmits power and torque from primary to secondary pulley shaft by means of friction developed between belt and pulley sheaves' contacts [27-28].

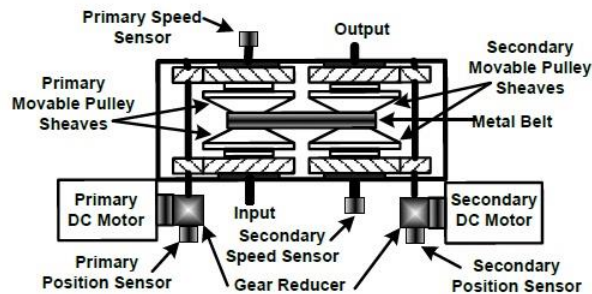


Figure 4 EMDAP CVT system

The EMDAP CVT system provides primary and secondary electro-mechanical actuating pulley sheaves (EMAPS) systems to actuate the movable pulley sheaves on its primary and secondary shaft, respectively. Each EMAPS mainly consists of DC motor system, gear reducer, two sets of helical gear reducers, two sets of power screw mechanisms and two movable pulley sheaves. The two gear reducers used in this application have a total gear ratio of 128:1. These gear reducers consist of a worm gearbox with ratio of 30:1, as shown in Fig. 5, and a helical gear system with ratio of 60:14.

The DC motor acts as a power source to actuate the EMAPS system, while the gearing system acts as speed reducer and torque multiplier for the DC motor to encounter power screw friction and belt clamping force. The input shaft of the gearing system is connected to the DC motor shaft, while the output of the gearing system actuates the power screw mechanisms to simultaneously shift the two movable pulley sheaves on each pulley shaft in

opposite direction to each other. This power screw mechanism converts every one rotational screw movement to about 2-millimeter axial movement. Each pulley sheave can travel up to 10 mm in order to obtain the smallest pulley gap. The helical gear systems and power screw mechanisms can be shown in Fig. 6. Narrowing the pulley gap increases belt-pulley radius and clamping force, while widening the pulley gap reduces belt-pulley radius and clamping force.



Figure 5 Gear reducer

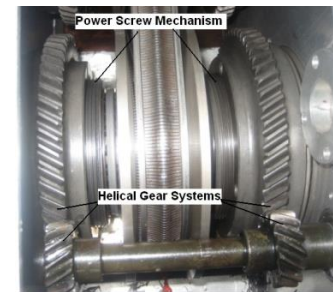


Figure 6 The helical gears and power screw mechanisms

By regulating the input voltage of the DC motor system, it is possible to adjust the axial pulley position accordingly. The pulley position represents the distance of the pulley sheave being shifted from its minimum position. Both primary and secondary axial pulley positions are directly measured using primary and secondary pulley position sensors. Based on these two pulley positions measurements, the pulley-belt running radii can be calculated using (6) and (7), and geometrical ratio of CVT can be determined using (2). When a new CVT ratio is required, both primary and secondary DC motors in EMAPS systems are controlled to shift the primary and secondary movable pulleys, respectively, to their new positions according to the graph given in Fig. 3. When the CVT ratio is achieved, the DC motors are turned off, and pulley positions are constantly locked by power screw mechanism.

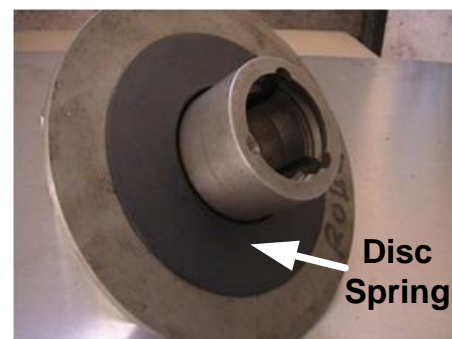


Figure 7 Disc spring on the back of secondary pulley sheave

In the secondary EMAPS system, a spring disc is inserted at the back of each secondary pulley sheave to keep the belt tight and prevent the belt slip, as shown in Fig. 7. Each disc spring can be flattened with a compression force of about 10 kN. The characteristic of the disc spring is shown in Fig. 8. Since there are two spring discs used in this system, the maximal force developed from the two spring discs are about 20 kN. The secondary DC motor system delivers sufficient belt-pulley clamping force to prevent belt slip by controlling the flatness of the spring discs [29]. During ratio calibration process, when the desired ratio is achieved, the spring discs are then fully flattened by the secondary DC motor.

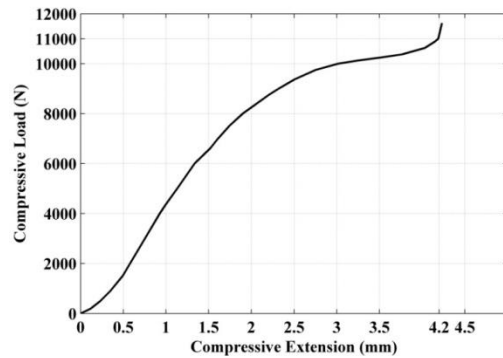


Figure 8 Characteristic of disc spring

4.0 EXPERIMENTAL TEST RIG

Experimental test rig was set up to carry out experimental works for ratio calibration of EMDAP CVT system. Block diagram of the test rig is shown in Fig. 9, while the photograph is shown in Fig. 10. The test rig of EMDAP CVT system consists of position sensors, speed sensors, DC motor drivers, DC motors, Data Acquisition Card, desktop computer, Matlab/Simulink software, power supply unit and AC motor. The DC motors are supplied using car battery of 24 V/70 Ah. An additional battery charger is provided to back up the battery capacity during experiment. The desktop computer, together with data acquisition card and Matlab/Simulink software is used to actuate the DC motors, read, calculate and record pulley positions, shaft speeds and CVT ratio from the respective sensors.

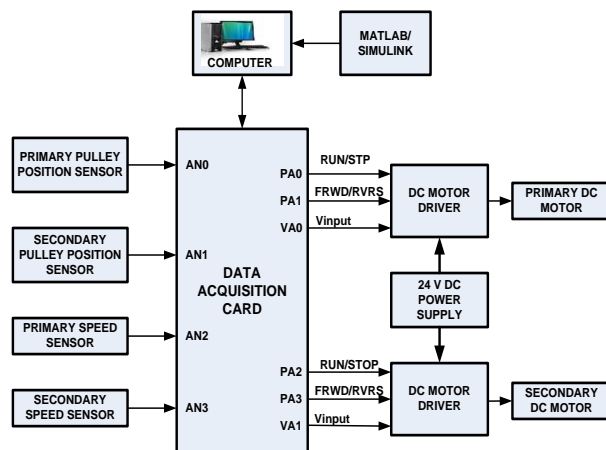


Figure 9 Block diagram of experimental test rig

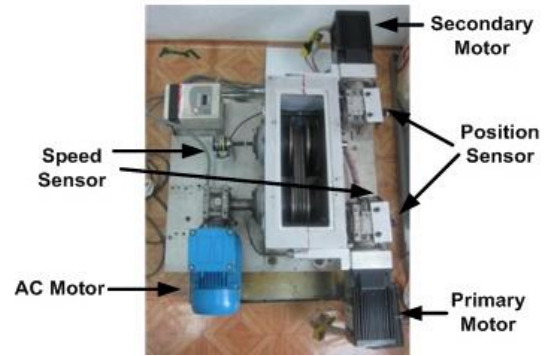


Figure 10 Photograph of the test rig

This research uses a three-phase alternative Current (AC) motor of 0.5 kW, shown in Fig. 10, as a power source to rotate the input shaft of the EMDAP CVT system. Output shaft of the AC motor is connected to the input of the speed reducer gearbox having ratio 1:30 to increase the output torque of the speed reducer gearbox by 30 times and decrease the speed of the reducer gearbox also by 30 times. The output of the speed reducer gearbox is connected to the input shaft of the EMDAP CVT. The speed of the AC motor is constantly set to 1700 rpm, hence the speed of the primary shaft on the EMDAP CVT is 56.66 rpm.

5.0 CALIBRATION PROCEDURE

5.1 Position Sensor

Each position sensor utilizes a 10-turn potentiometer to indirectly measure the axial displacement of pulley sheaves which have been shifted along its pulley shaft from its minimum position. The physical appearance of the position sensor is shown in Fig. 11. The position sensor is attached to the pinion shaft via a spur gear set having ratio of 16:42 as shown in Fig. 12. The shaft of the 16-tooth gear is coupled with the pinion shaft, while the shaft of the 42-tooth gear is fixed to the position sensor shaft. Since the gear ratio of the helical gear to move the power screw mechanism is 60:14, by referring to pinion shaft rotation (n_1), the rotation ratio between position sensor shaft (n_2) and power screw (n_3) can be calculated to be 240:147 or 1.63:1. In order to reach the maximum axial position of 10 mm, the power screw should rotate 5 times. Consequently, the effective rotation of the potentiometer is 8.17. Since the maximum rotation of position sensor shaft is 10, approximately two extra rotations are still left for safety reason to prevent the position sensor from damage due to overturn. Output voltage of position sensor is linearly proportional to the number of its shaft rotations. The specification of this sensor is 0.5 rotations/Volt. Two pulley positions are required to detect primary and secondary axial pulley positions. By using (2), the geometrical ratio of secondary to primary radii can be determined.



Figure 11 Position sensor

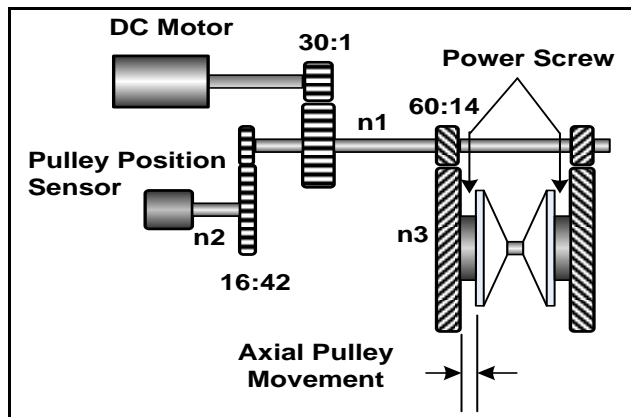


Figure 12 Pulley position sensor arrangement

5.2 Speed Sensor

Speed sensors are used to measure the rotational speeds of input and output shafts of the EMDAP CVT. The speed sensor uses rotational encoder, shown in Fig. 13, which gives 500 pulses per revolution to represent the angular speed of the shaft. The frequency of this angular speed is converted to its respective voltage by using frequency to voltage converter unit having specification of 18 rpm per volt, for maximum speed of 90 rpm. By using (3), the primary to secondary speed ratio can be determined.



Figure 13 Speed sensor

5.3 CVT Ratio

The calibration procedure for CVT ratio can be carried out as follows. Firstly, the AC motor is turned on to rotate the primary shaft at about 57 rpm. Then, the desired geometrical ratio of secondary to primary radii is set manually by controlling the primary and secondary DC motor systems to adjust the primary and secondary axial pulley positions according to the graph shown in Fig. 3. The real speed ratio is calculated by dividing the input shaft speed with the output shaft speed resulted from speed measurements, and displayed on the computer screen. When the desired geometrical ratio has achieved the same value as that of the speed ratio, the AC motor is stopped, and the CVT ratio has been obtained. The current primary and secondary pulley widths, L_{xp} and L_{xs} , respectively, are measured using digital Vernier Caliper as shown in Fig. 14. The relationship between pulley width and axial pulley positions are presented as follows:

$$X_p = (L_{xp0} - L_{xp})/2 \quad (8)$$

$$X_s = (L_{xs0} - L_{xs})/2 \quad (9)$$

where, L_{xp0} and L_{xs0} are the widths of primary and secondary pulley gaps when their axial positions are zero. By using (8) and (9), the axial pulley positions can be obtained. Then by using (6) and (7) pulley radii can be calculated, and using (2) the geometrical ratio of secondary to primary radii can be determined.

This experiment was carried out for CVT ratio from 0.7 to 2.0 with the step increment of 0.05. The corresponding values of primary and secondary pulley positions, output voltages of pulley position sensors as well as output voltages of shaft speed sensors are recorded and used as reference data for future EMDAP CVT calibration process before it is used for real control implementation.

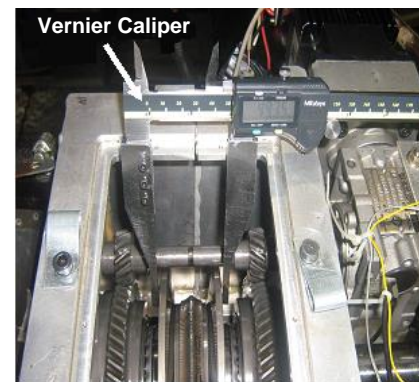


Figure 14 Pulley gap measurement

6.0 RESULTS AND DISCUSSION

The results presented are based on the data obtained from several experiments performed using data acquisition system and MATLAB/Simulink software. The software reads and saves the output voltages of axial primary and secondary pulley position sensors as well as the output voltages of primary and secondary speed sensors. Based on these voltage data, calculations were performed to determine the actual measurement values of axial pulley positions, pulley radii, shaft speeds and CVT ratios.

Based on experimental works, the relationship between output voltage of primary position sensor and primary axial pulley position is shown in Fig. 15, while the relationship between output voltage of secondary position sensor and secondary axial pulley position is shown in Fig. 16. The results show linear relationships between the output voltages of position sensors and their respective axial pulley positions; hence the actual axial pulley position measurements and calculations performed by computer can be carried out easily and accurately.

When the CVT ratio value increases from 0.7 to 2.0, the secondary shaft speed decreases from approximately 80 to 28 rpm. The same speed is achieved when the CVT ratio is one, which is 1:1 ratio. If the CVT ratio is less than one, then the secondary speed is bigger than the primary speed. The fastest secondary speed occurs when the CVT ratio is 0.7, which is called as an over-drive ratio. But, if the CVT ratio is bigger than one, then the secondary speed is less than the primary speed. The slowest speed occurs when the CVT ratio is 2.0, which is an under-drive ratio. For all CVT ratios (0.7 to 2.0), the average values of primary and secondary speeds are shown in Fig. 17, while the output voltages of primary and secondary pulley position sensors are displayed in Fig. 18.

The effective working ranges of the primary and secondary pulley position sensors are approximately of 0.7 to 3.4 and 0.5 to 3.1 Volts, respectively. Maximum voltages of primary and

secondary pulley position sensors are about 3.4 and 3.1 Volts respectively, which are less than 5 Volt. It means that both position sensors are working in the safe region, since their working ranges never exceeds 5 Volt.

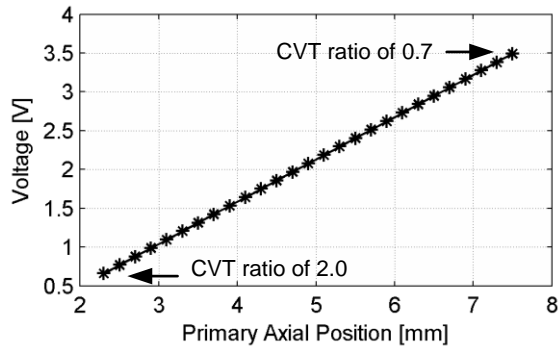


Figure 15 Output voltage of primary position sensor

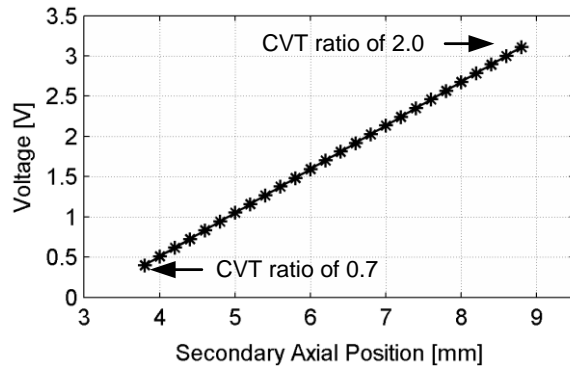


Figure 16 Output voltage of secondary position sensor

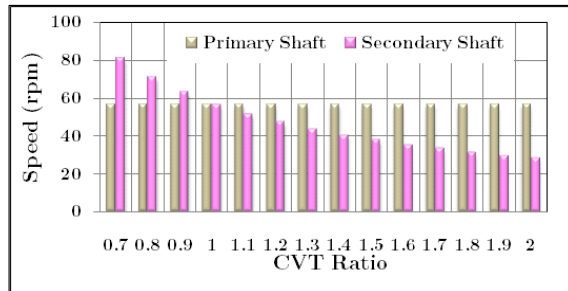


Figure 17 Shaft speeds vs. CVT ratio

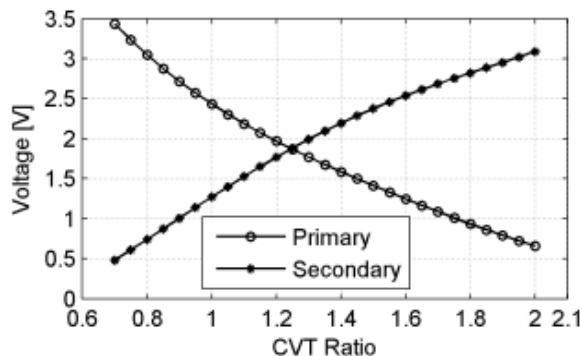


Figure 18 Output voltage of position sensors vs. CVT ratio

6.0 CONCLUSION

The experimental rig has been set up and validation of CVT ratio of 0.7 to 2.0 based on the geometrical ratio of secondary to primary radii and primary to secondary speed ratio has been carried out successfully. The CVT ratio is achieved by matching the values of the geometrical ratio and the speed ratio by adjusting the primary and secondary pulley positions using DC motor systems. Pulley gap measurement can be used to obtain the actual pulley position that has a linear relationship with the output voltage of position sensor. The results of this calibration will be later used for future calibrations and ratio control developments.

Acknowledgement

We are grateful for UTM funding through University's Potential Academic Staff (PAS) research grant year 2013 to Bambang Supriyo.

References

- [1] S.A. Shaheen and T.E. Lipman. 2007. Reducing greenhouse emissions and fuel consumption-sustainable approaches for surface transportation. *Latss Research*. 31(1): 1–20.
- [2] U.F. Akpan and G.E. Akpan. 2012. The contribution of energy consumption to climate change: a feasibility policy direction. *International Journal of Energy Economics and Policy*. 2(1): 21–33.
- [3] N. Lutsei and D. Sperling. 2006. Energy efficiency, Fuel Economy, and policy implications. *Journal of the Transportation Research Board*. 1941: 8–17.
- [4] R. Jayabalan and A. Emadi. 2014. Acceleration Support by Integrated Starter/Alternator for Automotive Applications. *Proc. IMechE, Part D: Journal of Automobile Engineering*. 218 (1): 987–993.
- [5] C.P. Cooney, J.J. Worm and J.D. Naber. 2009. Combustion Characterization in an Internal Combustion Engine with Ethanol-Gasoline Blended Fuels Varying Compression Ratios and Ignition Timing. *Energy Fuels*. 23 (5): 2319–2324.
- [6] J. Szybist, M. Foster, W. Moore, K. Confer, A. Youngquist and R. Wagner. 2010. Investigation of knock limited compression ratio of ethanol gasoline blends. *SAE Technical Paper*. 01–0619.
- [7] R. Daniel, G. Tian, H. Xu and S. Shuai. 2012. Ignition timing sensitivities of oxygenated biofuels compared to gasoline in a direct-injection SI engine. *Fuel*. 99:72–82.
- [8] K. Kornbluth, J. Greenwood, Z. McCaffrey, D. Vernon and P. Erickson. 2010. Extension of the lean limit through hydrogen enrichment of a LFG-fueled spark-ignition engine and emissions reduction. *International Journal of Hydrogen Energy*. 35 (3): 1412–1419.
- [9] R.G. Shyani and J. A. Caton. 2009. A thermodynamic analysis of the use of exhaust gas recirculation in spark ignition engines including the second law of thermodynamics. *Proceedings of the Institution of Mechanical Engineers, Part D: Journal of Automobile Engineering*. 223 (1):131–149.
- [10] R. Daniel, C. Wang, H. Xu and G. Tian. 2012. Effects of Combustion Phasing, Injection Timing, Relative Air-Fuel Ratio and Variable Valve Timing on SI Engine Performance and Emissions using 2, 5-Dimethylfuran. *SAE International Journal of Fuels and Lubricant*. 5 (2): 855–866.
- [11] J.E. Negrete. 2010. *Effects of different fuels on a turbocharged, direct injection, spark ignition engine*. PhD diss., Massachusetts Institute of Technology.
- [12] T. Ide. 2000. Effect of Belt Loss and Oil Pump Loss on the Fuel Economy of a Vehicle with a Metal V-Belt CVT. *In Seoul 2000 FISITA World Automotive Congress*. Seoul, Korea.
- [13] H. Lee and H. Kim. 2003. CVT Ratio Control for Improvement of Fuel Economy by Considering Powertrain Response Lag. *KSME International Journal*. 17 (11):1725–173.
- [14] T. Doi. 2010. New compact, lightweight, low friction CVT with wide ratio changed after damaging the belt-pulley contact surfaces coverage. *Proc. of the 6th Int. Conf. on Continuously Variable and Hybrid Transmission*. Maastricht, Netherlands.
- [15] J.D. Micklem, D.K. Longmore, and C.R. Burrows. 1996. The magnitude of the losses in the steel pushing V-belt continuously variable transmission. *Proc. IMechE., Part D: Journal of Automobile Engineering*. 210 (1): 57–62.

- [16] B. Matthes. 2005. Dual Clutch Transmission-Lessons Learned and Future Potential. *SAE Technical Paper Series*. 01–1021.
- [17] T.W.G.L. Klaassen. 2007. *The Impact CVT; Dynamics and Control Of An Electromechanically Actuated CVT*. PhD Thesis. Library Eindhoven University of Technology.
- [18] W. Xudong, Z. Meilan and Z. Yongqin. 2006. Research on Electronic Control System of a New-type CVT. *IEEE Proceedings on the 1st International Forum on Strategic Technology (IFOST 2006)*. Ulsan, Korea. 289–292.
- [19] Y. Xinhua, C. Naishi and L. Zhaohui. 2008. Electro-Mechanical Control Devices for Continuously Variable Transmission. *SAE International Powertrains, Fuels and Lubricants Congress*. SAE 2008–01–1687.
- [20] B. Supriyo, K. B. Tawi, H. Jamaluddin, A. Budianto and I. I. Mazali. 2012. Shifting Performance Fuzzy-PID Ratio Controller of Electro-Mechanical Continuously Variable Transmission. *The 3rd International Conference on Circuits, Systems, Control, Signals, WSEAS, Barcelona, Spain*. 272–277.
- [21] K.B. Tawi, I.I. Mazali, B. Supriyo, N.A. Husain, M. Hussein, M.S.C. Kob and Y.Z. Abidin. 2013. Independent Clamping Actuator for Electro-Mechanical Continuously Variable Transmission. *Latest Trends in Circuits, Control and Signal Processing, Proc. 13th International Conference on Instrumentation, Measurement, Circuits and Systems (IMCAS '13)*. Kuala Lumpur, Malaysia. 33–37.
- [22] M.A.M. Dzahir, M. Hussein, K.B. Tawi, M.S. Yaacob, B. Supriyo, M.Z. M. Zain, M.S.C. Kob and M.A.M. Dzahir. 2013. System Identification of Electromechanical Dual Acting Pulley Continuously Variable Transmission (EMDAP CVT). *Computational Methods in Science and Engineering, Proc. 15th International Conference on Mathematical and Computational Methods in Science and Engineering (MACMESE '13)*. Kuala Lumpur, Malaysia. 105–110.
- [23] F. Zang. 2009. Study of The Electro-Hydraulic Control System for CVT Metal Belt Axial-Misalignment. *International Conference on Mechatronics and Automation (ICMA 2009)*. Changchun, China. 1531–1535.
- [24] F. Zang and Z. Wu. 2009. Control Study on the CVT Metal V-belt's Axial-Misalignment of Car. *IEEE Intelligent Vehicles Symposium*. Xi'an, Shaanxi, China.
- [25] F. Zang. 2010. Simulation and Fuzzy Control Study on the CVT Metal V Belt Axial Misalignment of Car. *Key Engineering Materials*. 426–427 (1): 97–101.
- [26] B. Supriyo, K.B. Tawi, M. Hussein, I.I. Mazali, M.S.C. Kob, M. Azwarie and Y. Z. Abidin. 2013. Ratio Calibration of Electro-Mechanical Dual Acting Pulley Continuously Variable Transmission System. *Latest Trends in Circuits, Control and Signal Processing, Proc. 13th International Conference on Instrumentation, Measurement, Circuits and Systems (IMCAS '13)*. Kuala Lumpur, Malaysia. 38–43.
- [27] T.W.G.L. Klaassen, B. Bonsen, K.G.O. van de Meerakker, M. Steinbuch, P.A. Veenhuizen and F.E. Veldpaus. 2004. Nonlinear Stabilization of Slip in a Continuously Variable Transmission. *IEEE International Conference on Control Applications*. Taipei, Taiwan.
- [28] K. van Berkel, T. Fujii, T. Hofman and M. Steinbuch. 2011. Belt-Pulley Friction Estimation for the Continuously Variable Transmission. *The 50th IEEE Conference on Decision and Control and European Control Conference (CDC-ECC)*. Orlando, FL, USA.
- [29] B. Supriyo, K.B. Tawi and H. Jamaluddin. 2013. Experimental Study of an Electromechanical CVT Ratio Controller System. *International Journal of Automotive Technology*. 14 (2): 313–323.